Atmospheric Chemistry and Physics Discussions

Quantification of hydroxyacetone and glycolaldehyde using chemical ionization mass spectrometry

K. M. Spencer[1]**, M. R. Beaver**[2]**, J. M. St. Clair**[2]**, J. D. Crounse**[2]**, F. Paulot**[3]**, and P. O. Wennberg**[2,3]

[1]Division of Chemistry and Chemical Engineering, California Institute of Technology, Pasadena, CA, USA
[2]Division of Geological and Planetary Sciences, California Institute of Technology, Pasadena, CA, USA
[3]Division of Engineering and Applied Science, California Institute of Technology, Pasadena, CA, USA

Correspondence to: K. M. Spencer (kspencer@caltech.edu)

Title Page

Abstract	Introduction
Conclusions	References
Tables	Figures

|◄ | ►|
◄ | ►

Back | Close

Full Screen / Esc

Printer-friendly Version

Interactive Discussion

Abstract

Chemical ionization mass spectrometry (CIMS) enables online, fast, in situ detection and quantification of hydroxyacetone and glycolaldehyde. Two different CIMS approaches are demonstrated employing the strengths of single quadrupole mass spectrometry and triple quadrupole (tandem) mass spectrometry. Both methods are capable of the measurement of hydroxyacetone, an analyte with minimal isobaric interferences. Tandem mass spectrometry provides direct separation of the isobaric compounds glycolaldehyde and acetic acid using distinct, collision-induced dissociation daughter ions. Measurement of hydroxyacetone and glycolaldehyde by these methods was demonstrated during the ARCTAS-CARB 2008 campaign and the BEARPEX 2009 campaign. Enhancement ratios of these compounds in ambient biomass burning plumes are reported for the ARCTAS-CARB campaign. BEARPEX observations are compared to simple photochemical box model predictions of biogenic volatile organic compound oxidation at the site.

1 Introduction

Carbonyl compounds make a large contribution to the production of free radicals and photooxidants in the atmosphere. Hydroxyacetone ($H_3CC(O)CH_2OH$) and glycolaldehyde ($HC(O)CH_2OH$) have both biogenic and biomass burning sources. Both species are important oxidation products of isoprene (2-methyl-1,3-butadiene), and glycolaldehyde is also produced during the oxidation of 2-methyl-3-buten-2-ol (MBO). Isoprene is produced by deciduous plants and is the single largest source of nonmethane hydrocarbons to the atmosphere (Guenther et al., 1995) while MBO is emitted in large quantities from several species of pine (Goldan et al., 1993; Harley et al., 1998). Isoprene undergoes photooxidation to produce methyl vinyl ketone (MVK) and methacrolein (MACR) (Tuazon and Atkinson, 1990a; Paulson et al., 1992). MVK and MACR are further oxidized to produce second-generation isoprene photooxidation products

K. M. Spencer et al.

glycolaldehyde, hydroxyacetone, methylglyoxal ($H_3CC(O)CH(O)$), and formaldehyde (CH_2O) (Tuazon and Atkinson, 1989, 1990b). Recent studies suggest additional prompt sources of hydroxyacetone and glycolaldehyde during the isomerization of alkoxyradicals formed from isoprene photooxidation (Dibble, 2004a,b; Paulot et al., 2009a; Karl et al., 2009; Galloway et al., 2011). Hydroxyacetone and glycolaldehyde are also emitted during biomass burning. Christian et al. (2003) quantified hydroxyacetone and glycolaldehyde in laboratory fires of Indonesian and African fuels, and Bertschi et al. (2003) observed glycolaldehyde in emissions of laboratory fires of downed logs, duff, and organic soils.

Hydroxyacetone and glycolaldehyde are precursors of other atmospherically relevant species. Major products of hydroxyacetone and glycolaldehyde photooxidation are methylglyoxal and glyoxal (OCHCHO), respectively (Grosjean et al., 1993; Niki et al., 1987). Additionally, Butkovskaya et al. (2006a,b) found oxidation of hydroxyacetone and glycolaldehyde by OH yields formic acid while OH oxidation of hydroxyacetone also produces acetic acid. Oxidation products of biogenic volatile organic compounds play a significant role in tropospheric ozone production (Chameides et al., 1988; Atkinson and Arey, 2003) and formation of secondary organic aerosol (Kroll et al., 2006).

Previous measurements of hydroxyacetone and glycolaldehyde concentrations have been made using a range of analytical techniques. The most common of these involve ambient sample collection, derivatization with a chemical agent, separation of compounds, and detection by HPLC, GC-MS, or GC-FID (Lee et al., 1993, 1995; Zhou et al., 2009; Moortgat et al., 2002; Spaulding et al., 2003; Matsunaga et al., 2003). Two shortcomings of these techniques are the intensive sample processing required and the time lag between sample collection and concentration measurement. In contrast, both single quadrupole and triple quadrupole (tandem) chemical ionization mass spectrometry enable online, fast, in situ measurements with no sample processing. In these techniques, the ambient sample enters the instrument directly and reaches the detector in less than one second, enabling immediate detection of these compounds. The Caltech single quadrupole and tandem chemical ionization mass spectrometers are

equally capable of quantifying hydroxyacetone, an analyte with minimal known isobaric interferences. The Caltech tandem chemical ionization mass spectrometer enables direct separation of mass analogues glycolaldehyde and acetic acid. A similar method, proton-transfer-reaction mass spectrometry (PTRMS), has been used recently by Karl et al. (2009) to measure hydroxyacetone concentrations in the Amazon basin.

We present in situ measurements of hydroxyacetone and glycolaldehyde in the boundary layer of California and at a tower site approximately 80 km northeast of Sacramento, California. The first set of measurements was made in June of 2008 from the NASA DC-8 aircraft platform using the Caltech single quadrupole chemical ionization mass spectrometry (CIMS) instrument during the California portion of the NASA-CARB Arctic Research of the Composition of the Troposphere from Aircraft and Satellites (ARCTAS-CARB) field experiment. The four ARCTAS-CARB flights included in this study (18, 20, 22, and 26 June) occurred during daytime hours. Enhancement ratios of hydroxyacetone and glycolaldehyde in biomass burning plumes are presented and compared to literature values for laboratory fire data.

The second set of measurements was made during the Biosphere Effects on Aerosols and Photochemistry Experiment (BEARPEX) 2009 field experiment from 28 June to 20 July using the Caltech tandem CIMS instrument. The site is a ponderosa pine plantation (38°53′42.9″ N, 120°37′57.9″ W, elevation 1315 m), located near the University of California's Blodgett Forest Research Station, on the western slope of the Sierra Nevada. The site is approximately five hours downwind of Sacramento and has been described in detail previously by Goldstein et al. (2000) and Dreyfus et al. (2002). The measurements presented here were conducted from the top platform of the north tower; the instrument inlet was located 17.8 m above the ground. Concentrations of hydroxyacetone and glycolaldehyde are compared to results from a simple photochemical box model used to estimate the contribution of biogenic sources to the budget of glycolaldehyde and hydroxyacetone at the site.

2 Instrumentation

2.1 Instrument description

Negative ion chemistry of CF_3O^- has been shown to provide sensitive detection of many atmospheric trace gases (Huey et al., 1996; Amelynck et al., 2000a,b; Crounse et al., 2006; Spencer et al., 2009; Paulot et al., 2009b; St. Clair et al., 2010) and was exploited in this work to detect hydroxyacetone, glycolaldehyde, and acetic acid. The use of CF_3O^- to detect hydroxyacetone and glycolaldehyde was introduced briefly by Paulot et al. (2009a) and Chan et al. (2009) and is described in detail here. Hydroxyacetone and glycolaldehyde react with CF_3O^- via clustering between the reagent ion and the analyte through Reactions (R1) and (R2), respectively. Acetic acid reacts with CF_3O^- via fluoride ion transfer through Reaction (R3) and clustering through Reaction (R4), providing two distinct ion signals. Reactions (R1)–(R4) are complicated by competing reactions with CF_3O^- water cluster ($CF_3O^- \cdot H_2O$).

$$CF_3O^- + H_3CC(O)CH_2OH \rightarrow CF_3O^- \cdot H_3CC(O)CH_2OH \ \ (m/z \ 159) \quad\quad\quad (R1)$$

$$CF_3O^- + HC(O)CH_2OH \rightarrow CF_3O^- \cdot HC(O)CH_2OH \ \ (m/z \ 145) \quad\quad\quad (R2)$$

$$CF_3O^- + H_3CC(O)OH \rightarrow H_3CC(O)O^- \cdot HF \ \ (m/z \ 79) + CF_2O \quad\quad\quad (R3)$$

$$CF_3O^- + H_3CC(O)OH \rightarrow CF_3O^- \cdot H_3CC(O)OH \ \ (m/z \ 145) \quad\quad\quad (R4)$$
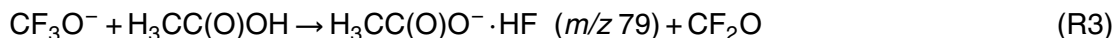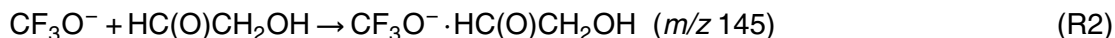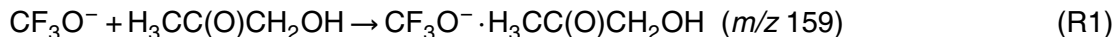
Hydroxyacetone and glycolaldehyde measurements were made using the Caltech single quadrupole CIMS instrument and the Caltech tandem CIMS instrument. The Caltech single quadrupole CIMS instrument consists of a flow tube controlled at 35 hPa total pressure, where a reagent ion, CF_3O^-, interacts with ambient air diluted 1:4 with ultra high purity N_2. Ions are sampled from the flow tube into a quadrupole mass filter and detected with a channel electron multiplier. Each mass-to-charge ratio is observed for $\sim$0.5 s. Hydroxyacetone, glycolaldehyde, and acetic acid masses were monitored once every $\sim$15 s. As in the Caltech single quadrupole CIMS instrument,

Title Page

Abstract Introduction

Conclusions References

Tables Figures

◄◄ ►►

◄ ►

Back Close

Full Screen / Esc

Printer-friendly Version

Interactive Discussion

the flow tube of the Caltech tandem CIMS instrument is maintained at 35 hPa total pressure. During the BEARPEX campaign, ambient air was diluted 1:7 with liquid nitrogen boil off. The Caltech tandem CIMS instrument contains three quadrupoles. The first quadrupole filters ions for a specific mass-to-charge ratio. These ions then enter the second quadrupole, which serves as a collision-induced dissociation (CID) chamber. The pressure in this quadrupole is maintained at 2.7×10^{-3} hPa N_2. Ions that reach this chamber collide with N_2 molecules and fragment into daughter ions. The third quadrupole selects for a specific daughter ion. Each mass-to-charge ratio is observed for ~1 s. Hydroxyacetone, glycolaldehyde, and acetic acid masses were monitored once every ~25 s. Further details on the Caltech single quadrupole and tandem CIMS instruments are given in Crounse et al. (2006) and St. Clair et al. (2010), respectively.

2.2 Calibration and sensitivity

Due to differences in the reactivity of the analyte with CF_3O^- and $CF_3O^- \cdot H_2O$, the sensitivity of the Caltech CIMS instrumentation to the ion products of Reactions (R1)–(R4) varies with the mixing ratio of water vapor present in the flow tube. H_2O can also displace or hydrolyze the analyte anion. The dependence of instrument sensitivity on water vapor mixing ratio was quantified during laboratory calibrations, in which a known quantity of analyte was added to the flow tube. The ion signal was determined as a function of humidity to obtain a water-dependent sensitivity curve. In all calibrations, mass flow controllers were used to control the flow tube humidity by adjusting the ratio of moist N_2 to dry N_2. Humidity was quantified by Fourier Transform Infrared (FTIR) spectroscopy using HITRAN line lists (Rothman et al., 2005) and the nonlinear fitting software NLM4 developed by Griffith (1996). All analyte sensitivities were corrected for background signals.

For calibrations, hydroxyacetone and glycolaldehyde standards were prepared by serial dilution, and an acetic acid permeation tube was used. Gas-phase hydroxyacetone was produced by flowing dry N_2 over commercially available, 95 % pure

Full Screen / Esc

Printer-friendly Version

Interactive Discussion

hydroxyacetone (Alfa Aesar) into a 150 l Teflon bag. Additional dry N_2 was added to the bag such that the final concentration of hydroxyacetone was 150 ppmv. Initially, the hydroxyacetone concentration was determined by both FTIR absorption (Orlando et al., 1999) and quantification of the mass loss of the liquid. These methods agreed within
5   25 %; the concentration determined by mass loss was higher than that determined by FTIR absorption. In calibration experiments, hydroxyacetone concentration was determined by mass loss alone as the FTIR absorption instrument was dedicated to the determination of water vapor concentration. 150 ml from the 150 l bag were quantitatively transferred to a 400 l Teflon bag. A known quantity of dry N_2 was added such that
10   the concentration of hydroxyacetone was 50 ppbv. Similarly, gas-phase glycolaldehyde was transferred to a 100 l Teflon bag by flowing dry N_2 over commercially available glycolaldehyde dimer (Fluka Analytical) while gently heating the compound. Additional dry N_2 was added to the bag such that the concentration of glycolaldehyde was 100 ppmv. Similarly to hydroxyacetone, the glycolaldehyde concentration was determined by both
15   FTIR absorption (Tuazon and Atkinson, 1989) and quantification of the mass loss of the solid. These methods agreed within 45 %; the concentration determined by mass loss was higher than that determined by FTIR absorption. In calibration experiments, glycolaldehyde concentration was determined by mass loss alone as the FTIR absorption instrument was dedicated to the determination of water vapor concentration. 300 ml
20   from the 100 l bag were quantitatively transferred to a 400 l Teflon bag. A known quantity of dry N_2 was added such that the concentration of glycolaldehyde was 75 ppbv. A ^{13}C isotopically labeled acetic acid standard was used. The acetic acid evolved from a permeation tube that was held at a constant temperature (Washenfelder et al., 2003), and the permeation rate was determined by mass loss.
25   Calibrations of hydroxyacetone, glycolaldehyde, and acetic acid were conducted separately, but the method was similar for all calibrations. A known quantity of analyte from the standards discussed above was combined with water vapor and N_2 dilution gas in the instrument flow tube. The CIMS instrument signal was monitored as a function of water vapor in the flow tube to develop the instrument sensitivity curve.

The sensitivity of the single quadrupole CIMS instrument to the cluster channel of hydroxyacetone (*m/z* 159), the cluster channel of glycolaldehyde (*m/z* 145), the fluoride transfer channel of acetic acid (*m/z* 79), and the cluster channel of acetic acid (*m/z* 145) is shown in red, green, blue, and black, respectively, in Fig. 1. The sensitivity of the tandem CIMS instrument to the hydroxyacetone daughter ion (m159m85), glycolaldehyde daughter ion (m145m85), acetic acid fluoride transfer daughter ion (m79m59), and acetic acid cluster daughter ion (m145m79) is shown in red, green, blue, and black, respectively, in Fig. 2. Daughter ions produced in the CID chamber of the Caltech tandem CIMS instrument are discussed below in Sect. 3.2. Sensitivity is expressed in ion counts, normalized by the ion counts of the ^{13}C or ^{17}O isotope of the reagent ion and its one-water cluster, per pptv of analyte. Daughter ions m86m86, m104m86, and m104m104 of the reagent ions are used in normalization of the tandem CIMS instrument ion counts.

Postmission laboratory calibrations for hydroxyacetone, glycolaldehyde, and acetic acid were conducted for both the single quadrupole CIMS instrument and the tandem CIMS instrument. During the ARCTAS-CARB flights and the BEARPEX experiment, isotopically labeled acetic acid from the permeation tube was periodically added to the flow tube of the CIMS instruments to quantify the instrument sensitivity. The sensitivity of the single quadrupole CIMS instrument to acetic acid during the ARCTAS-CARB campaign was consistent with that of postmission laboratory calibrations. The consistent sensitivity of the tandem CIMS instrument was similarly confirmed during the BEARPEX campaign and postmission laboratory calibrations.

In the absence of hydroxyacetone, glycolaldehyde, and acetic acid, ion signals at *m/z* 159, *m/z* 145, and *m/z* 79 are nonzero, and these background signals must be accounted for in the data analysis. Background signals were measured during flight by periodically passing ambient air through a filter consisting of a few alumina pellets coated with palladium followed by nylon wool coated with sodium bicarbonate, quantitatively removing hydroxyacetone, glycolaldehyde, and acetic acid. This technique is described in Crounse et al. (2006). Background signals were monitored approximately

every 20 min during the ARCTAS-CARB flights and approximately every 45 min during the BEARPEX campaign. The measured background signals are used to model background levels during data collection.

3 Determination of analyte concentration

3.1 Single quadrupole CIMS instrument

The single quadrupole CIMS instrument was used to conduct ambient measurements in and around California during the ARCTAS-CARB campaign. Determination of the analyte ion signal of hydroxyacetone, glycolaldehyde, and acetic acid is discussed below. Ambient concentrations of these trace gases are calculated from the analyte ion signal after normalization by the amount of reagent ion signal, subtraction of background signals, and application of the appropriate sensitivity factor.

3.1.1 Hydroxyacetone

As discussed above, hydroxyacetone clusters with the reagent ion CF_3O^- and is detected at *m/z* 159. The uncertainty in the single quadrupole hydroxyacetone measurements is approximately ±(30 % of the measurement value + 50 pptv). The uncertainty reflects the sum of the precision of the data determined by the counting statistics of the ions, the variability of the background signal, and the uncertainty in the sensitivity factor shown in Fig. 1. Propanoic acid is also observed at this mass, but its concentration is low (Yokelson et al., 2009) and is not expected to be a significant interference in the hydroxyacetone signal.

3.1.2 Glycolaldehyde

The quantification of glycolaldehyde is complicated by a significant interference due to acetic acid, an exact mass analogue of glycolaldehyde. Both species undergo CF_3O^- clustering chemistry and are detected at *m/z* 145. Thus, the *m/z* 145 signal due to

acetic acid in the form $CF_3O^- \cdot H_3CC(O)OH$ must be accounted for when determining the ambient glycolaldehyde concentration. This is accomplished by estimating the *m/z* 145 acetic acid signal from the acetic acid signal detected at *m/z* 79.

As discussed above, acetic acid also reacts with CF_3O^- via fluoride ion transfer and
5 is detected as $H_3CC(O)O^- \cdot HF$ at *m/z* 79 (R3). There are no known interferences at this mass-to-charge ratio. The ratio of fluoride transfer ions (*m/z* 79) to clustering ions (*m/z* 145) for acetic acid is dependent on the amount of water in the instrument flow tube (Fig. 1). The ratio is determined experimentally via the laboratory and field calibrations discussed above. The *m/z* 145 signal due to acetic acid is estimated by
10 multiplying the *m/z* 79 acetic acid signal by the water-dependent ratio of the acetic acid *m/z* 145 signal to the acetic acid *m/z* 79 signal. The average acetic acid contribution to the *m/z* 145 signal ranged from 40 % to 60 % of the total *m/z* 145 signal for the four ARCTAS-CARB flights. The contribution of acetic acid and glycolaldehyde to the *m/z* 145 signal are shown for the 18 June 2008 flight in Fig. 3.

15 The *m/z* 145 signal due to glycolaldehyde is calculated by subtracting the *m/z* 145 signal due to acetic acid from the total *m/z* 145 signal detected by the single quadrupole CIMS instrument. The corrected glycolaldehyde signal is converted to concentration by application of the laboratory-determined instrument sensitivity factor for glycolaldehyde (Fig. 1, green curve). The uncertainty in the single quadrupole glycolaldehyde
20 measurements is approximately ±(60 % + 50 pptv). The uncertainty reflects the sum of the precision of the data determined by the counting statistics of the ions, the variability of the background signal, the uncertainty in the sensitivity factor shown in Fig. 1, and the uncertainty in acetic acid attribution.

3.2 Tandem CIMS instrument

25 The tandem CIMS instrument was used to conduct ambient measurements at a tower site about five hours downwind of Sacramento during the BEARPEX 2009 campaign. Determination of the analyte ion signals of hydroxyacetone, glycolaldehyde, and acetic acid is discussed below. Similar to measurements made using the single quadrupole

instrument, ambient concentrations of these trace gases are calculated from the ion signals after normalization by the amount of reagent ion signal, subtraction of background signals, and application of the appropriate sensitivity factor. An advantage of tandem CIMS lies in the ability to differentiate between isobaric species provided their fragmentation patterns are sufficiently different.

3.2.1 Hydroxyacetone

Tandem mass spectrometry measurement of hydroxyacetone is similar to that of single quadrupole mass spectrometry. The hydroxyacetone daughter ion signal at m/z 85 (m159m85) was used. The uncertainty in the tandem hydroxyacetone measurements is approximately $\pm(30\% + 50\,\text{pptv})$. The uncertainty reflects the sum of the precision of the data determined by the counting statistics of the ions, the variability of the background signal, and the uncertainty in the sensitivity factor shown in Fig. 2.

3.2.2 Glycolaldehyde

The advantages of tandem mass spectrometry are demonstrated in the separate quantification of isobaric compounds glycolaldehyde and acetic acid. The sequence of quadrupole mass filter, collision-induced dissociation (CID) chamber, and second quadrupole mass filter enables the decomposition of isobaric ions into daughter ion fragments. As discussed above, while operating in tandem MS mode, ions of a selected mass-to-charge ratio pass through the first quadrupole mass filter and into the CID chamber, where they collide with N_2 molecules and fragment into daughter ions. The second quadrupole mass filter selects daughter ions of a certain mass-to-charge ratio.

Glycolaldehyde and acetic acid CF_3O^- cluster ions fragment differently due to differences in the stabilities of their clusters and the resultant daughter fragments. Significant daughter ion signals were observed at m/z 79, m/z 85, and m/z 145 and are denoted m145m79, m145m85, and m145m145, respectively. Figure 4 shows the parent

ions – glycolaldehyde and acetic acid – and their significant daughter ion fragments. The daughter ion signals are reported relative to the sum of the three significant daughter ion signals for each compound. As shown in Fig. 4a, 90 % of glycolaldehyde m/z 145 parent ions fragment to m/z 85 daughter ions, and zero percent fragment to m/z 79 daughter ions. The predominate daughter ion of acetic acid m/z 145 parent ions is m/z 79 (72 %) (Fig. 4b). Ten percent of acetic acid m/z 145 parent ions fragment to m/z 85. 10 % of glycolaldehyde and 18 % of acetic acid m/z 145 parent ions do not fragment and are detected at m145m145. These percentages are too similar to enable unambiguous determination of the two species using m145m145 daughter ions. Acetic acid also fragments to m145m59, but the ion signal is a factor of ten less than that observed at m145m79.

Based on these fragmentation patterns, ambient signals due to glycolaldehyde and acetic acid are separated. The m145m85 signal is mainly due to glycolaldehyde, and the small contribution due to acetic acid is accounted for during data analysis. The signal at m145m85 due to acetic acid is calculated by multiplying the acetic acid signal at m145m79 by the laboratory-derived ratio of acetic acid signal at m145m85 to acetic acid signal at m145m79. The m145m85 signal due to glycolaldehyde is calculated by subtracting the acetic acid m145m85 signal from the total m145m85 signal.

Final glycolaldehyde concentrations are calculated using the corrected glycolaldehyde m145m85 ion signal and the corresponding tandem CIMS instrument sensitivity curve. Final acetic acid concentrations are calculated using both the m79m59 and m145m79 ion signals and their respective sensitivity curves. The uncertainty in the tandem glycolaldehyde measurements is approximately ±(50 % + 50 pptv). The uncertainty in the tandem acetic acid measurements is approximately ±(40 % + 50 pptv). The uncertainties reflect the sum of the precision of the data determined by the counting statistics of the ions, the variability of the background signal, and the uncertainty in the sensitivity factors shown in Fig. 2.

4 Observations

Aircraft observations indicate a range of hydroxyacetone and glycolaldehyde concentrations in California. Low altitude (<1.5 km pressure altitude) DC-8 flight tracks over northern and central California colored by observed hydroxyacetone concentrations are
5 shown in Fig. 5a. Observed concentrations range from several hundred pptv along the coast to concentrations greater than 2 ppbv further inland, closer to biomass burning and biogenic sources. Flight tracks colored by observed glycolaldehyde concentrations are shown in Fig. 5b. Similar to hydroxyacetone concentrations, glycolaldehyde concentrations are low along the coast and much greater (>10 ppbv) closer to biomass
10 burning and biogenic sources.

Ground-based measurements of hydroxyacetone, glycolaldehyde, and acetic acid concentrations during BEARPEX 2009 are shown in Fig. 6; ambient temperature is shown also. The average ambient temperature was ∼5 K higher for days after Day of Year (DOY) 195 compared to those prior. This is a likely explanation for the increase
15 in observed hydroxyacetone, glycolaldehyde, and acetic acid concentrations after DOY 195 as emissions of isoprene and MBO are light and temperature dependent (Baker et al., 1999; Lamanna et al., 1999; Schade et al., 2000; Schade and Goldstein, 2001; Gray et al., 2005).

5 Results and discussion

20 ### 5.1 ARCTAS-CARB 2008

Hydroxyacetone and glycolaldehyde concentrations are well correlated with hydrogen cyanide (HCN) during the ARCTAS-CARB 2008 campaign. Fig. 7 shows the correlation between glycolaldehyde and HCN in blue and the correlation between hydroxyacetone and HCN in red. Data shown are low altitude measurements (<1.5 km pressure altitude). Linear regression, using the York et al. (2004) method that takes into account
25

errors in both the abscissa and ordinate values, gives a slope of 2.5 and 0.48, respectively. $R^2 = 0.84$ and 0.77, respectively. HCN is an atmospheric tracer of biomass burning emissions (e.g., Li et al., 2003) and was also measured during the ARCTAS-CARB campaign using the Caltech single quadrupole CIMS instrument (Crounse et al., 2009). Significant hydroxyacetone and glycolaldehyde concentrations occur only in airmasses with elevated HCN ($\geq$250 pptv). In 2003, Christian et al. reported major, previously unobserved hydroxyacetone and glycolaldehyde emissions from combustion of Indonesian and African fuels during laboratory studies.

Emission ratios and enhancement ratios are commonly used to describe biomass burning emissions. An enhancement ratio or normalized excess mixing ratio typically takes the form $\Delta[X]/\Delta[Y]$, where X and Y are two species present in the smoke plume. $\Delta[X]$ is the enhancement of the mixing ratio of X in the plume compared to the mixing ratio of X in background air. ΔY is usually a long-lived plume tracer such as ΔCO or ΔCO_2 (Yokelson et al., 2007). As the plumes analyzed in this work were not nascent plumes (age ranged from several minutes to one day) (Hornbrook et al., 2011), enhancement ratios rather than emission ratios are presented.

Enhancement ratios relative to CO for hydroxyacetone, glycolaldehyde, and HCN were calculated for plumes of biomass burning origin encountered during ARCTAS-CARB and were compared to previous field and laboratory findings. Many previous studies have determined emission or enhancement ratios of HCN from biomass burning; few studies have reported enhancement ratios for hydroxyacetone and glycolaldehyde.

Individual enhancement ratios were calculated for three biomass burning plumes in which hydroxyacetone, glycolaldehyde, HCN, and CO were measured. A list of biomass burning plumes encountered by the DC-8 during the ARCTAS campaign can be found in Hornbrook et al. (2011). Possible biomass burning plumes are identified by time periods of elevated biomass burning tracer mixing ratios. Plumes are defined by HCN greater than 400 pptv, acetonitrile (CH_3CN) greater than 200 pptv, and CO greater than 175 ppbv. Elevated mixing ratios of NO_x and toluene, anthropogenic tracers, were

used to exclude plumes sampled in urban regions. Multiple samplings of a plume were grouped together and are referred to as a single plume. The plumes analyzed in this work were encountered at UTC 18:27–18:30 and 18:38–18:41 on 18 June, 21:08–21:12 and 21:23–21:44 on 22 June, and 14:32–14:35, 15:34–16:17, and 16:39–16:57 on 26 June. The correlation of the species of interest (hydroxyacetone, glycolaldehyde, or HCN) versus a long-lived plume tracer (CO) was determined by linear regression using the York et al. (2004) method. Calculated enhancement ratios, associated R^2 values, and plume age of the three plumes are given in Table 1.

There is substantial variability in HCN enhancement ratios with respect to CO. Using a total least-squares analysis method, Crounse et al. (2009) calculated an emission ratio of 9.6 HCN to CO (pptv ppbv^{-1}) in Mexico City. This is consistent with the median emission ratio value of 8.5 determined by Yokelson et al. (2007) for the same sampling region and time period. Singh et al. (2003) observed a mean HCN enhancement ratio of 3.4 during measurements of Asian pollution outflow in 2001. Enhancement ratios of HCN in biomass burning plumes encountered in California during ARCTAS-CARB range from 2.1 to 4.1 HCN to CO (pptv ppbv^{-1}) (Table 1). The variability in HCN enhancement ratios may be explained by differences in combustion conditions and fuel type (Yokelson et al., 2007).

Christian et al. (2003) measured glycolaldehyde and hydroxyacetone emission ratios during laboratory studies of Indonesian and African fuels. Using the emission ratio of CO, HCN, glycolaldehyde, and hydroxyacetone to CO_2 determined by Christian et al. (2003), corresponding emission ratios relative to CO were estimated. The emission ratio of HCN, glycolaldehyde, and hydroxyacetone relative to CO (pptv ppbv^{-1}) is 12.3, 6.4, and 22.1, respectively, in fires from Indonesian fuels and 8.6, 3.2, and 3.3, respectively, in fires from African savanna fuels. Mean calculated enhancement ratios of HCN, glycolaldehyde, and hydroxyacetone for the biomass burning plumes encountered in California and discussed in this work are 2.9, 5.7, and 1.5, respectively. These two sets of ratios were determined for fires of both different fuel and age. Post-emission chemistry is expected to affect enhancement ratios, and fuel type is likely an important

factor in the type and magnitude of emitted species. Nevertheless, the ARCTAS-CARB observations combined with previous laboratory observations demonstrate the range of emission ratios / enhancement ratios that may be measured from biomass burning sources.

5.2 BEARPEX 2009

The BEARPEX site is located on the western slope of the Sierra Nevada in a ponderosa pine plantation. The site is approximately five hours downwind of Sacramento, and a band of oak forests is located approximately halfway between Sacramento and the site. The prevailing daytime wind pattern transports anthropogenic volatile organic compounds (VOCs) and NO_x emissions from Sacramento and the Central Valley to the site. Isoprene, emitted from the band of oak forests, and MBO, emitted locally by the ponderosa pine forest, are added to the mixture. Wind direction reverses at night and brings clean air from the mountains to the site. Further details of the BEARPEX site can be found in Goldstein et al. (2000) and Dreyfus et al. (2002).

Hydroxyacetone and glycolaldehyde concentrations are well correlated during the BEARPEX 2009 campaign (Fig. 8). The slope of the linear regression is 1.300 ± 0.003, and the intercept is 0.70 ± 0.17 pptv. $R^2 = 0.91$. The remarkable correlation is consistent with the hypothesis that hydroxyacetone and glycolaldehyde have similar sources (isoprene second-generation photooxidation) and sinks (reaction with OH and photolysis). The mean hydroxyacetone concentration measured during BEARPEX 2009 was 774 pptv, and the mean glycolaldehyde concentration was 986 pptv. Spaulding et al. (2003) measured similar hydroxyacetone and glycolaldehyde concentrations (420 pptv and 690 pptv, respectively) during an eight-day sampling period at the same site in August and September of 2000.

Using a simple box model, the ratio of glycolaldehyde to hydroxyacetone at the BEARPEX site was calculated. VOCs represented in the model are isoprene and MBO; the concentrations of these VOCs simulate an isoprene source between Sacramento and the measurement site (the suburban oak tree belt) and a local source of MBO

from the ponderosa pine plantation. The model was developed such that emissions from Sacramento (located at time = 0) and the surburban oak tree belt (located at time ≈150 min) are processed en route to the BEARPEX site (located at time ≈300 min). The magnitude of the emissions is constructed such that the concentrations of iso-prene and MBO are consistent with measurements conducted at the site. 300 min is chosen as the time representative of the measurement site, consistent with a 5-hour transport time from Sacramento to the site. Modeled concentrations of isoprene and MBO are shown in Fig. 9a. At 300 min, isoprene and MBO concentrations are both 2 ppbv.

Reaction rate constants are taken from IUPAC (Atkinson et al., 2004, 2006) and JPL (Sander et al., 2006) compilations. The rate constant for the reaction of isoprene-derived RO_2 and HO_2 discussed in Jenkin et al. (1997) has been used. Photolysis rates were calculated using the Tropospheric Ultraviolet and Visible (TUV) radiation model (http://cprm.acd.ucar.edu/Models/TUV/). The isoprene oxidation mechanisms of Paulot et al. (2009a,b) have been followed with modifications and additions to mechanisms based on recent laboratory chamber experiments. The yield of hydroxyacetone from methacrolein oxidation in the presence of NO_x has been increased to 0.43 from 0.2 (Galloway et al., 2011). The mechanism describing MBO oxidation in the presence of NO_x from Chan et al. (2009) has been followed. A 0.15 yield of glycolaldehyde from MBO oxidation under low-NO_x conditions has been used as suggested by recent laboratory chamber experiments performed at Caltech. A unimolecular isomerization pathway from the hydroxyperoxy radical of MACR that yields hydroxyacetone has been added and is the dominant formation pathway for hydroxyacetone in the model. When this pathway is excluded from the model, hydroxyacetone formation is dominated by NO oxidation of MACR and resulting concentrations are much lower. The model includes a smaller yield of hydroperoxide from MVK oxidation followed by HO_2 chemistry (0.3) than recommended by the Master Chemical Mechanism, MCM v3.2 (Jenkin et al., 1997; Saunders et al., 2003) and a large yield (0.6) of glycolaldehyde. This simple model does not include deposition.

Absolute concentrations of glycolaldehyde and hydroxyacetone calculated by the model are 1.1 and 0.9 ppbv, respectively, at 300 min and are similar to the mean observations from the campaign. The ratio of the glycolaldehyde concentration to hydroxyacetone concentration predicted by the model is shown in Fig. 9b. The predicted ratio resulting from only isoprene oxidation ranges from 1.1 to 1.3. The initial ratio is determined by the prompt formation of glycolaldehyde and hydroxyacetone via radical rearrangement as proposed by theoretical work (Dibble, 2004a,b) and recent laboratory chamber experiments (Paulot et al., 2009a; Galloway et al., 2011) and suggested by field observations (Karl et al., 2009). The ratio increases when glycolaldehyde from MVK oxidation and hydroxyacetone from MACR oxidation are the dominant formation pathways. Since glycolaldehyde is formed from MBO oxidation and hydroxyacetone is not, the glycolaldehyde/hydroxyacetone ratio increases from 1.3 to 1.6 as more MBO is oxidized to form glycolaldehyde (250–600 min). The ratio of the production rate of glycolaldehyde to that of hydroxyacetone is shown in Fig. 9a and is mostly affected by increased glycolaldehyde production from MBO oxidation. Late in the model, oxidation of dihydroxyepoxides (IEPOX) of isoprene contributes to both hydroxyacetone and glycolaldehyde concentrations, highlighting the potential importance of the highly uncertain, late-generation isoprene oxidation chemistry at the site. The observed ratio of glycolaldehyde to hydroxyacetone at the BEARPEX site is 1.3 (Fig. 8), indicating predictions based only on isoprene and MBO chemistry are consistent with observations.

6 Conclusions

Chemical ionization mass spectrometry provides robust detection and quantification of hydroxyacetone and glycolaldehyde. The Caltech single quadrupole and tandem mass spectrometers are equally capable of the measurement of hydroxyacetone. Tandem mass spectrometry provides direct separation of the daughter ions of glycolaldehyde and acetic acid, enabling the differentiation of these mass analogues. This online method enables fast, in situ measurements with no sample processing.

Discussion Paper | Discussion Paper | Discussion Paper | Discussion Paper |

Ambient measurements of hydroxyacetone and glycolaldehyde were conducted during the ARCTAS-CARB 2008 campaign using the Caltech single quadrupole CIMS instrument. Enhancement ratios of hydroxyacetone, glycolaldehyde, and HCN were calculated for three biomass burning plumes encountered in California during June 2008. Ambient measurements of hydroxyacetone and glycolaldehyde concentrations from oxidation of biogenic emissions were conducted during the BEARPEX 2009 campaign using the Caltech tandem CIMS instrument. The observed ratio of measured glycolaldehyde concentration to measured hydroxyacetone concentration is consistent with predictions from a simplified box model in which isoprene and MBO are the only VOCs represented.

References

Amelynck, C., Schoon, N., and Arijs, E.: Gas phase reactions of CF_3O^- and $CF_3O^- \cdot H_2O$ with nitric, formic, and acetic acid, International J. Mass Spectrom., 203, 165–175, 2000. 23623

Amelynck, C., Van Bavel, A. M., Schoon, N., and Arijs, E.: Gas phase reactions of CF_3O^- and $CF_3O^- \cdot H_2O$ and their relevance to the detection of stratospheric HCl, International J. Mass Spectrom., 202, 207–216, 2000. 23623

Atkinson, R. and Arey, J.: Gas-phase tropospheric chemistry of biogenic volatile organic compounds: A review, Atmos. Environ., 37, S197–S219, doi:10.1016/S1352-2310(03)00391-1, 2003. 23621

Atkinson, R., Baulch, D. L., Cox, R. A., Crowley, J. N., Hampson, R. F., Hynes, R. G., Jenkin, M. E., Rossi, M. J., and Troe, J.: Evaluated kinetic and photochemical data for atmospheric

chemistry: Volume I – gas phase reactions of O_x, HO_x, NO_x and SO_x species, Atmos. Chem. Phys., 4, 1461–1738, doi:10.5194/acp-4-1461-2004, 2004. 23635

Atkinson, R., Baulch, D. L., Cox, R. A., Crowley, J. N., Hampson, R. F., Hynes, R. G., Jenkin, M. E., Rossi, M. J., Troe, J., and IUPAC Subcommittee: Evaluated kinetic and photochemical data for atmospheric chemistry: Volume II - gas phase reactions of organic species, Atmos. Chem. Phys., 6, 3625–4055, doi:10.5194/acp-6-3625-2006, 2006. 23635

Baker, B., Guenther, A., Greenberg, J., Goldstein, A., and Fall, R.: Canopy fluxes of 2-methyl-3-buten-2-ol over a ponderosa pine forest by relaxed eddy accumulation: Field data and model comparison, J. Geophys. Res.-Atmos., 104, 26107–26114, 1999. 23631

Bertschi, I., Yokelson, R. J., Ward, D. E., Babbitt, R. E., Susott, R. A., Goode, J. G., and Hao, W. M.: Trace gas and particle emissions from fires in large diameter and belowground biomass fuels, J. Geophys. Res.-Atmos., 108, 8472, doi:10.1029/2002JD002100, 2003. 23621

Butkovskaya, N. I., Pouvesle, N., Kukui, A., and Le Bra, G.: Mechanism of the OH-initiated oxidation of glycolaldehyde over the temperature range 233–296 K, J. Phys. Chem. A, 110, 13492–13499, doi:10.1021/JP064993K, 2006a. 23621

Butkovskaya, N. I., Pouvesle, N., Kukui, A., Mu, Y. J., and Le Bras, G.: Mechanism of the OH-initiated oxidation of hydroxyacetone over the temperature range 236–298 K, J. Phys. Chem. A, 110, 6833–6843, doi:10.1021/JP056345R, 2006b. 23621

Chameides, W. L., Lindsay, R. W., Richardson, J., and Kiang, C. S.: The role of biogenic hydrocarbons in urban photochemical smog: Atlanta as a Case Study, Science, 241, 1473–1475, 1988. 23621

Chan, A. W. H., Galloway, M. M., Kwan, A. J., Chhabra, P. S., Keutsch, F. N., Wennberg, P. O., Flagan, R. C., and Seinfeld, J. H.: Photooxidation of 2-Methyl-3-Buten-2-ol (MBO) as a Potential Source of Secondary Organic Aerosol, Environ. Sci. Technol., 43, 4647–4652, doi:10.1021/ES802560W, 2009. 23623, 23635

Christian, T. J., Kleiss, B., Yokelson, R. J., Holzinger, R., Crutzen, P. J., Hao, W. M., Saharjo, B. H., and Ward, D. E.: Comprehensive laboratory measurements of biomass-burning emissions: 1. Emissions from Indonesian, African, and other fuels, J. Geophys. Res.-Atmos., 108, 4719, doi:10.1029/2003JD003704, 2003. 23621, 23632, 23633

Crounse, J. D., DeCarlo, P. F., Blake, D. R., Emmons, L. K., Campos, T. L., Apel, E. C., Clarke, A. D., Weinheimer, A. J., McCabe, D. C., Yokelson, R. J., Jimenez, J. L., and Wennberg, P. O.: Biomass burning and urban air pollution over the Central Mexican Plateau, Atmos. Chem. Phys., 9, 4929–4944, doi:10.5194/acp-9-4929-2009, 2009. 23632, 23633

Quantification of hydroxyacetone and glycolaldehyde

K. M. Spencer et al.

Crounse, J. D., McKinney, K. A., Kwan, A. J., and Wennberg, P. O.: Measurement of gas-phase hydroperoxides by chemical ionization mass spectrometry, Anal. Chem., 78, 6726–6732, 2006. 23623, 23624, 23626

Dibble, T. S.: Intramolecular hydrogen bonding and double H-atom transfer in peroxy and alkoxy radicals from isoprene, J. Phys. Chem. A, 108, 2199–2207, doi:10.1021/JP0306702, 2004a. 23621, 23636

Dibble, T. S.: Prompt chemistry of alkenoxy radical products of the double H-atom transfer of alkoxy radicals from isoprene, J. Phys. Chem. A, 108, 2208–2215, doi:10.1021/JP0312161, 2004b. 23621, 23636

Dreyfus, G. B., Schade, G. W., and Goldstein, A. H.: Observational constraints on the contribution of isoprene oxidation to ozone production on the western slope of the Sierra Nevada, California, J. Geophys. Res.-Atmos., 107, 4365, doi:10.1029/2001JD001490, 2002. 23622, 23634

Galloway, M. M., Huisman, A. J., Yee, L. D., Chan, A. W. H., Loza, C. L., Seinfeld, J. H., and Keutsch, F. N.: Yields of oxidized volatile organic compounds during the OH radical initiated oxidation of isoprene, methyl vinyl ketone, and methacrolein under high-NO_x conditions, Atmos. Chem. Phys. Discuss., 11, 10693–10720, doi:10.5194/acpd-11-10693-2011, 2011. 23621, 23635, 23636

Goldan, P. D., Kuster, W. C., Fehsenfeld, F. C., and Montzka, S. A.: The Observation of a C_5 Alcohol Emission in a North American Pine Forest, Geophysical Research Letters, 20, 1039–1042, 1993. 23620

Goldstein, A. H., Hultman, N. E., Fracheboud, J. M., Bauer, M. R., Panek, J. A., Xu, M., Qi, Y., Guenther, A. B., and Baugh, W.: Effects of climate variability on the carbon dioxide, water, and sensible heat fluxes above a ponderosa pine plantation in the Sierra Nevada (CA), Agricultural and Forest Meteorology, 101, 113–129, 2000. 23622, 23634

Gray, D. W., Goldstein, A. H., and Lerdau, M. T.: The influence of light environment on photosynthesis and basal methylbutenol emission from *Pinus ponderosa*, Plant Cell Environ., 28, 1463–1474, 2005. 23631

Griffith, D. W. T.: Synthetic calibration and quantitative analysis of gas-phase FT-IR spectra, Appl. Spectrosc., 50, 59–70, 1996. 23624

Grosjean, D., Williams, E. L., and Grosjean, E.: Atmospheric chemistry of isoprene and of its carbonyl products, Environ. Sci. Technol., 27, 830–840, 1993. 23621

Guenther, A., Hewitt, C. N., Erickson, D., Fall, R., Geron, C., Graedel, T., Harley, P., Klinger, L.,

Quantification of hydroxyacetone and glycolaldehyde

K. M. Spencer et al.

Title Page

Abstract | Introduction

Conclusions | References

Tables | Figures

◄ | ►►

◄ | ►

Back | Close

Full Screen / Esc

Printer-friendly Version

Interactive Discussion

Lerdau, M., McKay, W. A., Pierce, T., Scholes, B., Steinbrecher, R., Tallamraju, R., Taylor, J., and Zimmerman, P.: A global-model of natural volatile organic-compound emissions, J. Geophys. Res.-Atmos., 100, 8873–8892, 1995. 23620

Harley, P., Fridd-Stroud, V., Greenberg, J., Guenther, A., and Vasconcellos, P.: Emission of 2-methyl-3-buten-2-ol by pines: A potentially large natural source of reactive carbon to the atmosphere, J. Geophys. Res.-Atmos., 103, 25479–25486, 1998. 23620

Hornbrook, R. S., Blake, D. R., Diskin, G. S., Fuelberg, H. E., Meinardi, S., Mikoviny, T., Sachse, G. W., Vay, S. A., Weinheimer, A. J., Wiedinmyer, C., Wisthaler, A., Hills, A., Riemer, D. D., and Apel, E. C.: Observations of volatile organic compounds during ARCTAS - Part 1: Biomass burning emissions and plume enhancements, Atmos. Chem. Phys. Discuss., 11, 14127–14182, doi:10.5194/acpd-11-14127-2011, 2011. 23632, 23644

Huey, L. G., Villalta, P. W., Dunlea, E. J., Hanson, D. R., and Howard, C. J.: Reactions of CF_3O^- with atmospheric trace gases, J. Phys. Chem., 100, 190–194, 1996. 23623

Jenkin, M. E., Saunders, S. M., and Pilling, M. J.: The tropospheric degradation of volatile organic compounds: A protocol for mechanism development, Atmos. Environ., 31, 81–104, 1997. 23635

Karl, T., Guenther, A., Turnipseed, A., Tyndall, G., Artaxo, P., and Martin, S.: Rapid formation of isoprene photo-oxidation products observed in Amazonia, Atmos. Chem. Phys., 9, 7753–7767, doi:10.5194/acp-9-7753-2009, 2009. 23621, 23622, 23636

Kroll, J. H., Ng, N. L., Murphy, S. M., Flagan, R. C., and Seinfeld, J. H.: Secondary organic aerosol formation from isoprene photooxidation, Environ. Sci. Technol., 40, 1869–1877, doi:10.1021/ES0524301, 2006. 23621

Lamanna, M. S. and Goldstein, A. H.: In situ measurements of C_2–C_{10} volatile organic compounds above a Sierra Nevada ponderosa pine plantation, J. Geophys. Res.-Atmos., 104, 21247–21262, 1999. 23631

Lee, Y. N. and Zhou, X. L.: Method for the determination of some soluble atmospheric carbonyl compounds, Environ. Sci. Technol., 27, 749–756, 1993. 23621

Lee, Y. N., Zhou, X. L., and Hallock, K.: Atmospheric carbonyl compounds at a rural Southeastern U.S. site, J. Geophys. Res.-Atmos., 100, 25933–25944, 1995. 23621

Li, Q. B., Jacob, D. J., Yantosca, R. M., Heald, C. L., Singh, H. B., Koike, M., Zhao, Y. J., Sachse, G. W., and Streets, D. G.: A global three-dimensional model analysis of the atmospheric budgets of HCN and CH_3CN: Constraints from aircraft and ground measurements, J. Geophys. Res.-Atmos., 108, 8827, doi:10.1029/2002JD003075, 2003. 23632

Quantification of hydroxyacetone and glycolaldehyde

K. M. Spencer et al.

Title Page

Abstract | Introduction

Conclusions | References

Tables | Figures

◄◄ | ►►

◄ | ►

Back | Close

Full Screen / Esc

Printer-friendly Version

Interactive Discussion

Matsunaga, S., Mochida, M., and Kawamura, K.: Growth of organic aerosols by biogenic semi-volatile carbonyls in the forestal atmosphere, Atmos. Environ., 37, 2045–2050, doi:10.1016/S1352-2310(03)00089-X, 2003. 23621

Moortgat, G. K., Grossmann, D., Boddenberg, A., Dallmann, G., Ligon, A. P., Turner, W. V., Gab, S., Slemr, F., Wieprecht, W., Acker, K., Kibler, M., Schlomski, S., and Bachmann, K.: Hydrogen peroxide, organic peroxides and higher carbonyl compounds determined during the BERLIOZ campaign, J. Atmos. Chem., 42, 443–463, 2002. 23621

Niki, H., Maker, P. D., Savage, C. M., and Hurley, M. D.: Fourier transform infrared study of the kinetics and mechanisms for the Cl-atom-initiated and HO-radical-initiated oxidation of glycolaldehyde, J. Phys. Chem., 91, 2174–2178, 1987. 23621

Orlando, J. J., Tyndall, G. S., Fracheboud, J. M., Estupinan, E. G., Haberkorn, S., and Zimmer, A.: The rate and mechanism of the gas-phase oxidation of hydroxyacetone, Atmos. Environ., 33, 1621–1629, 1999. 23625

Paulson, S. E., Flagan, R. C., and Seinfeld, J. H.: Atmospheric photooxidation of isoprene Part 1: The hydroxyl radical and ground-state atomic oxygen reactions, Int. J. Chem. Kin., 24, 79–101, 1992. 23620

Paulot, F., Crounse, J. D., Kjaergaard, H. G., Kroll, J. H., Seinfeld, J. H., and Wennberg, P. O.: Isoprene photooxidation: new insights into the production of acids and organic nitrates, Atmos. Chem. Phys., 9, 1479–1501, doi:10.5194/acp-9-1479-2009, 2009a. 23621, 23623, 23635, 23636

Paulot, F., Crounse, J. D., Kjaergaard, H. G., Kurten, A., St. Clair, J. M., Seinfeld, J. H., and Wennberg, P. O.: Unexpected Epoxide Formation in the Gas-Phase Photooxidation of Isoprene, Science, 325, 730–733, doi:10.1126/science.1172910, 2009b. 23623, 23635

Rothman, L. S., Jacquemart, D., Barbe, A., Benner, D. C., Birk, M., Brown, L. R., Carleer, M. R., Chackerian, C., Chance, K., Coudert, L. H., Dana, V., Devi, V. M., Flaud, J. M., Gamache, R. R., Goldman, A., Hartmann, J. M., Jucks, K. W., Maki, A. G., Mandin, J. Y., Massie, S. T., Orphal, J., Perrin, A., Rinsland, C. P., Smith, M. A. H., Tennyson, J., Tolchenov, R. N., Toth, R. A., Vander Auwera, J., Varanasi, P., and Wagner, G.: The HITRAN 2004 molecular spectroscopic database, J. Quant. Spectrosc. Ra., 96, 139–204, 2005. 23624

Sander, S. P., Friedl, R. R., Golden, D. M., Kurylo, M. J., Moortgat, G. K., Keller-Rudek, H., Wine, P. H., Ravishankara, A. R., Kolb, C. E., Molina, M. J., Finlayson-Pitts, B. J., Huie, R. E., and Orkin, V. L.: Chemical Kinetics and Photochemical Data for Use in Atmospheric Studies, Evaluation Number 15 JPL Publication 06-2, NASA Jet Propulsion Laboratory, California

Title Page

Abstract | Introduction

Conclusions | References

Tables | Figures

◄◄ | ►►

◄ | ►

Back | Close

Full Screen / Esc

Printer-friendly Version

Interactive Discussion

Institute of Technology, Pasadena, CA 2006. 23635

Saunders, S. M., Jenkin, M. E., Derwent, R. G., and Pilling, M. J.: Protocol for the development of the Master Chemical Mechanism, MCM v3 (Part A): tropospheric degradation of non-aromatic volatile organic compounds, Atmos. Chem. Phys., 3, 161–180, doi:10.5194/acp-3-161-2003, 2003. 23635

Schade, G. W. and Goldstein, A. H.: Fluxes of oxygenated volatile organic compounds from a ponderosa pine plantation, J. Geophys. Res.-Atmos., 106, 3111–3123, 2001. 23631

Schade, G. W., Goldstein, A. H., Gray, D. W., and Lerdau, M. T.: Canopy and leaf level 2-methyl-3-buten-2-ol fluxes from a ponderosa pine plantation, Atmos. Environ., 34, 3535–3544, 2000. 23631

Singh, H. B., Salas, L., Herlth, D., Kolyer, R., Czech, E., Viezee, W., Li, Q., Jacob, D. J., Blake, D., Sachse, G., Harward, C. N., Fuelberg, H., Kiley, C. M., Zhao, Y., and Kondo, Y.: In situ measurements of HCN and CH_3CN over the Pacific Ocean: Sources, sinks, and budgets, J. Geophys. Res.-Atmos., 108, 8795, doi:10.1029/2002JD003006, 2003. 23633

Spaulding, R. S., Schade, G. W., Goldstein, A. H., and Charles, M. J.: Characterization of secondary atmospheric photooxidation products: Evidence for biogenic and anthropogenic sources, J. Geophys. Res.-Atmos., 108, 4247, doi:10.1029/2002JD002478, 2003. 23621, 23634

Spencer, K. M., McCabe, D. C., Crounse, J. D., Olson, J. R., Crawford, J. H., Weinheimer, A. J., Knapp, D. J., Montzka, D. D., Cantrell, C. A., Hornbrook, R. S., Mauldin III, R. L., and Wennberg, P. O.: Inferring ozone production in an urban atmosphere using measurements of peroxynitric acid, Atmos. Chem. Phys., 9, 3697–3707, doi:10.5194/acp-9-3697-2009, 2009. 23623

St. Clair, J. M., McCabe, D. C., Crounse, J. D., Steiner, U., and Wennberg, P. O.: Chemical ionization tandem mass spectrometer for the in situ measurement of methyl hydrogen peroxide, Rev. Sci. Instrum., 81, 094102, doi:10.1063/1.3480552, 2010. 23623, 23624

Tuazon, E. C. and Atkinson, R.: A product study of the gas-phase reaction of methyl vinyl ketone with the OH radical in the presence of NO_x, Int. J. Chem. Kin., 21, 1141–1152, 1989. 23621, 23625

Tuazon, E. C. and Atkinson, R.: A product study of the gas-phase reaction of isoprene with the OH radical in the presence of NO_x, Int. J. Chem. Kin., 22, 1221–1236, 1990a. 23620

Tuazon, E. C. and Atkinson, R.: A product study of the gas-phase reaction of methacrolein with the OH radical in the presence of NO_x, Int. J. Chem. Kin., 22, 591–602, 1990b. 23621

Quantification of hydroxyacetone and glycolaldehyde

K. M. Spencer et al.

Washenfelder, R. A., Roehl, C. M., McKinney, K. A., Julian, R. R., and Wennberg, P. O.: A compact, lightweight gas standards generator for permeation tubes, Rev. Sci. Instrum., 74, 3151–3154, doi:10.1063/1.1570949, 2003. 23625

Yokelson, R. J., Urbanski, S. P., Atlas, E. L., Toohey, D. W., Alvarado, E. C., Crounse, J. D., Wennberg, P. O., Fisher, M. E., Wold, C. E., Campos, T. L., Adachi, K., Buseck, P. R., and Hao, W. M.: Emissions from forest fires near Mexico City, Atmos. Chem. Phys., 7, 5569–5584, doi:10.5194/acp-7-5569-2007, 2007. 23632, 23633

Yokelson, R. J., Crounse, J. D., DeCarlo, P. F., Karl, T., Urbanski, S., Atlas, E., Campos, T., Shinozuka, Y., Kapustin, V., Clarke, A. D., Weinheimer, A., Knapp, D. J., Montzka, D. D., Holloway, J., Weibring, P., Flocke, F., Zheng, W., Toohey, D., Wennberg, P. O., Wiedinmyer, C., Mauldin, L., Fried, A., Richter, D., Walega, J., Jimenez, J. L., Adachi, K., Buseck, P. R., Hall, S. R., and Shetter, R.: Emissions from biomass burning in the Yucatan, Atmos. Chem. Phys., 9, 5785–5812, doi:10.5194/acp-9-5785-2009, 2009. 23627

York, D., Evensen, N. M., Martinez, M. L., and Delgado, J. D.: Unified equations for the slope, intercept, and standard errors of the best straight line, Am. J. Phys., 72, 367–375, doi:10.1119/1.1632486, 2004. 23631, 23633

Zhou, X. L., Huang, G., Civerolo, K., and Schwab, J.: Measurement of Atmospheric Hydroxyacetone, Glycolaldehyde, and Formaldehyde, Environ. Sci. Technol., 43, 2753–2759, doi:10.1021/ES803025G, 2009. 23621

Title Page

Abstract	Introduction
Conclusions	References
Tables	Figures

|◀ | ▶|

◀ | ▶

Back | Close

Full Screen / Esc

Printer-friendly Version

Interactive Discussion

Table 1. Calculated enhancement ratios and the associated R^2 values (given in parentheses) of HCN, glycolaldehyde (GLYC), and hydroxyacetone (HAC) relative to long-lived plume tracer CO for three biomass burning plumes encountered during the ARCTAS-CARB campaign. The ratio of glycolaldehyde to hydroxyacetone in the plumes is included to enable comparison of the ratio of these compounds from biomass burning emissions and that of biogenic emissions, as measured during the BEARPEX 2009 campaign.

Flight Date	$\frac{\Delta HCN(pptv)}{\Delta CO(ppbv)}$		$\frac{\Delta GLYC(pptv)}{\Delta CO(ppbv)}$		$\frac{\Delta HAC(pptv)}{\Delta CO(ppbv)}$		$\frac{\Delta GLYC(pptv)}{\Delta HAC(pptv)}$		Plume Age (Days)[*]
18 June	4.1	(0.99)	4.6	(0.91)	1.6	(0.98)	2.8	(0.88)	1
22 June	2.1	(0.93)	5.7	(0.56)	1.5	(0.77)	3.4	(0.52)	0.1
26 June	2.4	(0.96)	6.8	(0.93)	1.3	(0.96)	5.2	(0.94)	1

[*] Hornbrook et al. (2011).
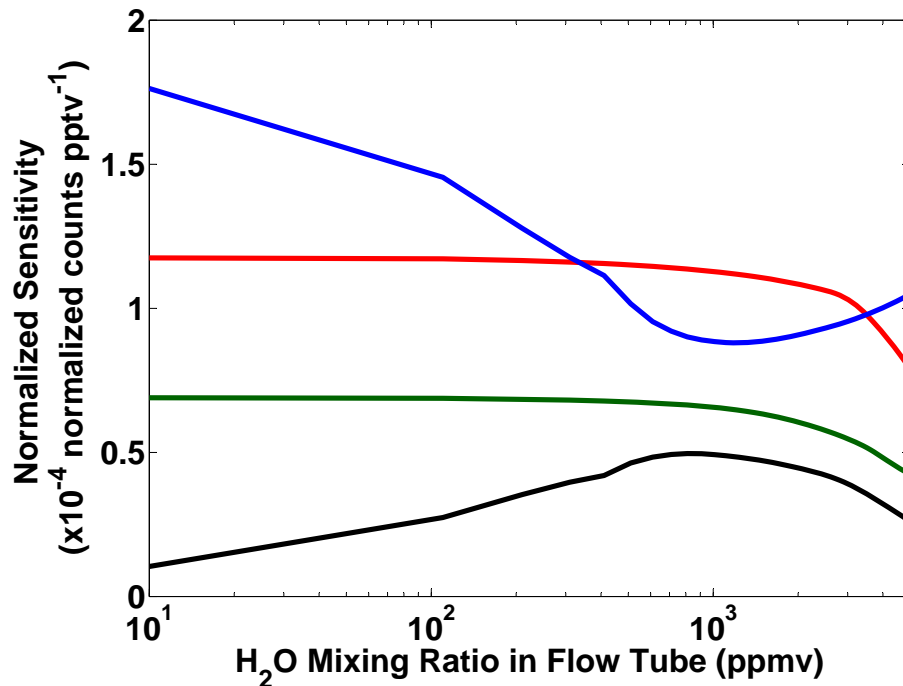
Fig. 1. Single quadrupole CIMS instrument sensitivity curves for hydroxyacetone (red), glycolaldehyde (green), acetic acid fluoride transfer product (blue), and acetic acid cluster product (black) as a function of H_2O mixing ratio in the instrument flow tube. The sensitivity curves are used to calculate the final concentrations of the analytes. Typical H_2O mixing ratio values in the instrument flow tube were approximately 1500 ppmv during the ARCTAS-CARB campaign.
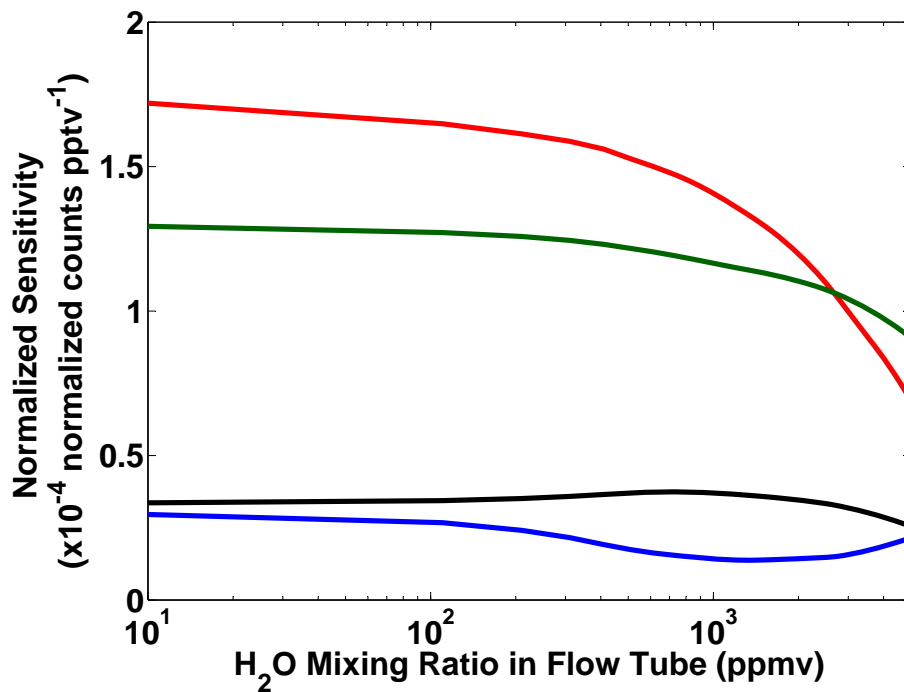
Fig. 2. Tandem CIMS instrument sensitivity curves for hydroxyacetone daughter ion m159m85 (red), glycolaldehyde daughter ion m145m85 (green), acetic acid fluoride transfer daughter ion m79m59 (blue), and acetic acid cluster daughter ion m145m79 (black) as a function of H_2O mixing ratio in the instrument flow tube. The sensitivity curves are used to calculate the final concentrations of the analytes. Typical H_2O mixing ratio values in the instrument flow tube were approximately 1500 ppmv during the BEARPEX campaign.
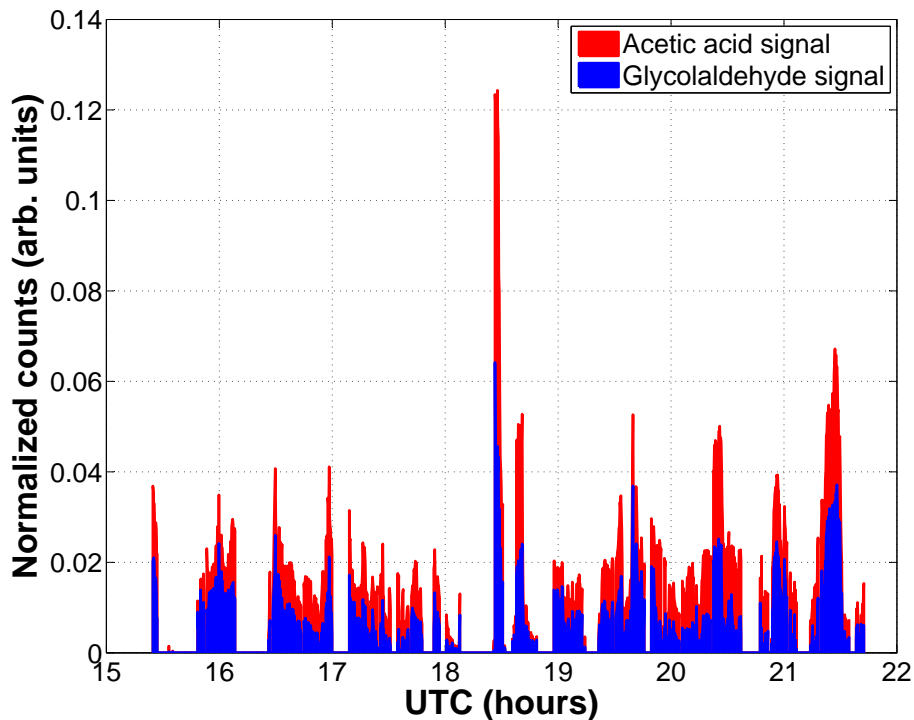
Fig. 3. A time series of the contribution of acetic acid and glycolaldehyde to the *m/z* 145 signal detected by the Caltech single quadrupole CIMS instrument during the 18 June 2008 flight. The *m/z* 145 signal due to acetic acid is estimated from the *m/z* 79 acetic acid signal. The signal due to glycolaldehyde is determined by subtracting the signal due to acetic acid from the total *m/z* 145 signal.

Full Screen / Esc

Printer-friendly Version

Interactive Discussion

A.

$CF_3O^-\cdot$ H–C(=O)–CH$_2$–OH   m/z 145

0% ↙   90% ↘

H–C(=O)–CH$_2$–O$^-\cdot$ HF
m/z 79

CF$_3$O$^-$
m/z 85

B.

$CF_3O^-\cdot$ H$_3$C–C(=O)–OH   m/z 145

72% ↙   10% ↘

H$_3$C–C(=O)–O$^-\cdot$ HF
m/z 79

CF$_3$O$^-$
m/z 85
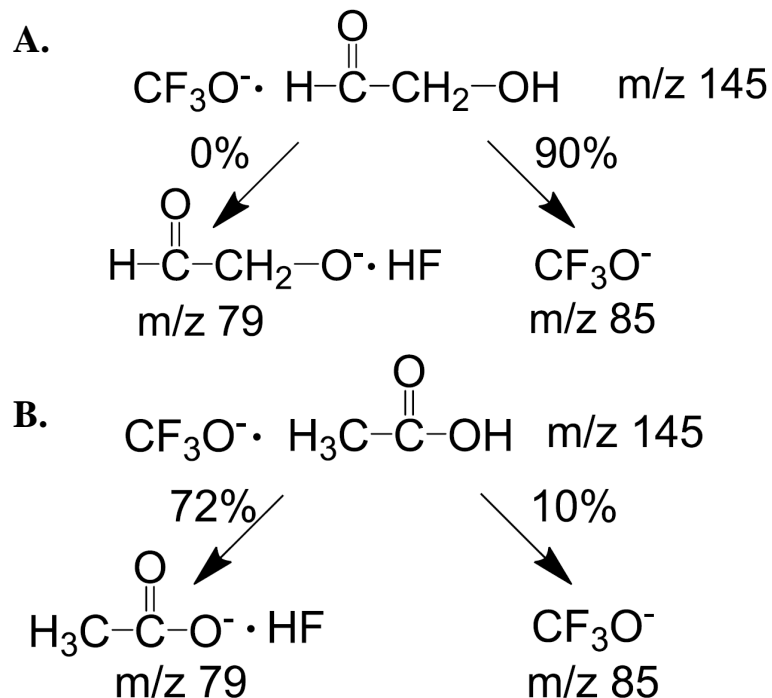
Fig. 4. Collision-induced dissociation fragmentation pattern of glycolaldehyde **(A)** and acetic acid **(B)** including the percentage of *m/z* 145 parent ions that fragment to each of the daughter ions. The excellent separation of daughter ions enables the differentiation of glycolaldehyde and acetic acid.
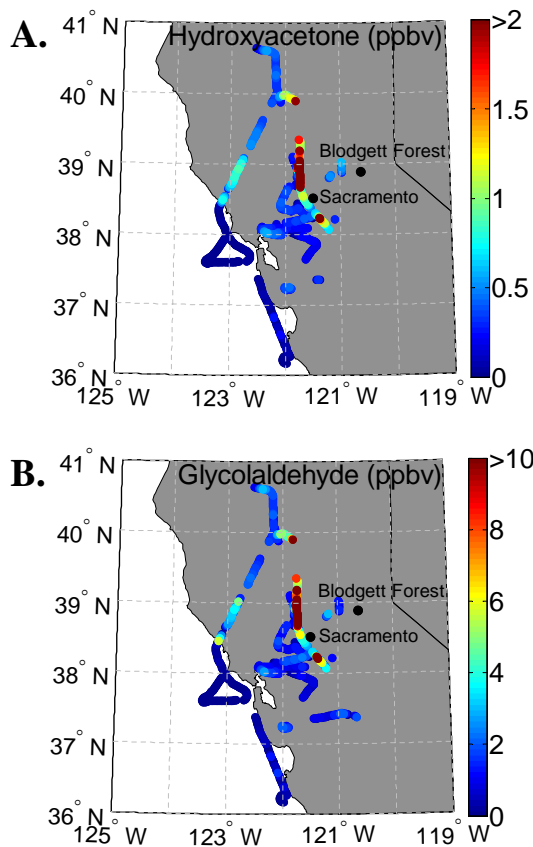
Fig. 5. ARCTAS-CARB flight tracks colored by hydroxyacetone **(A)** and glycolaldehyde **(B)**. Data presented are those when pressure altitude is less than 1.5 km. Observed concentrations of hydroxyacetone and glycolaldehyde are lowest along the coast and highest further inland, closer to biomass burning and biogenic sources.

Title Page

Abstract | Introduction

Conclusions | References

Tables | Figures

|◄ | ►|

◄ | ►

Back | Close

Full Screen / Esc

Printer-friendly Version

Interactive Discussion
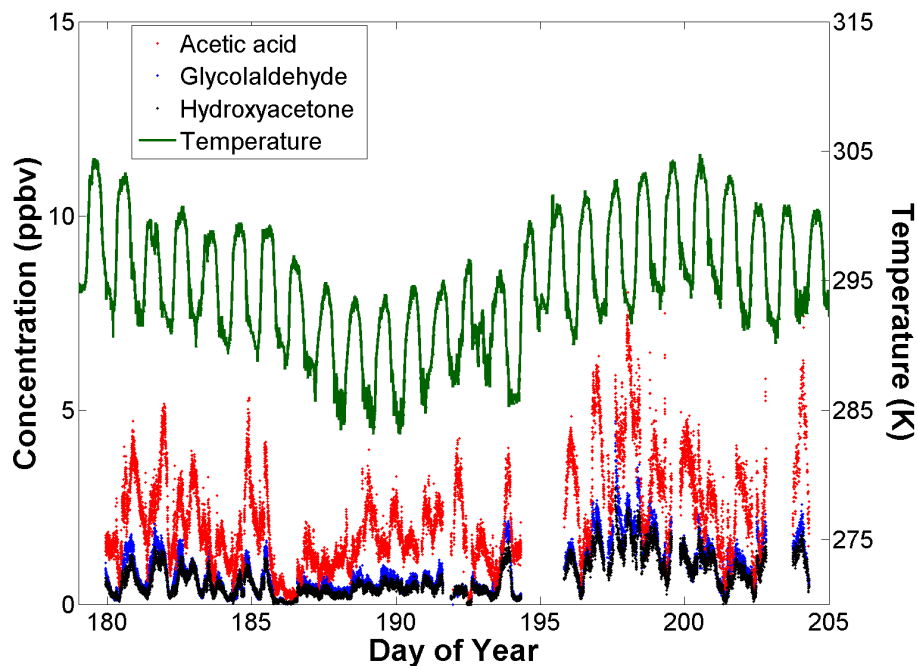
Fig. 6. Concentrations of acetic acid (m145m79), glycolaldehyde (m145m85), and hydroxyacetone (m159m85) measured using the Caltech tandem CIMS instrument during the BEARPEX 2009 campaign.

Title Page

Abstract   Introduction

Conclusions   References

Tables   Figures

◄   ►►

◄   ►

Back   Close

Full Screen / Esc

Printer-friendly Version

Interactive Discussion
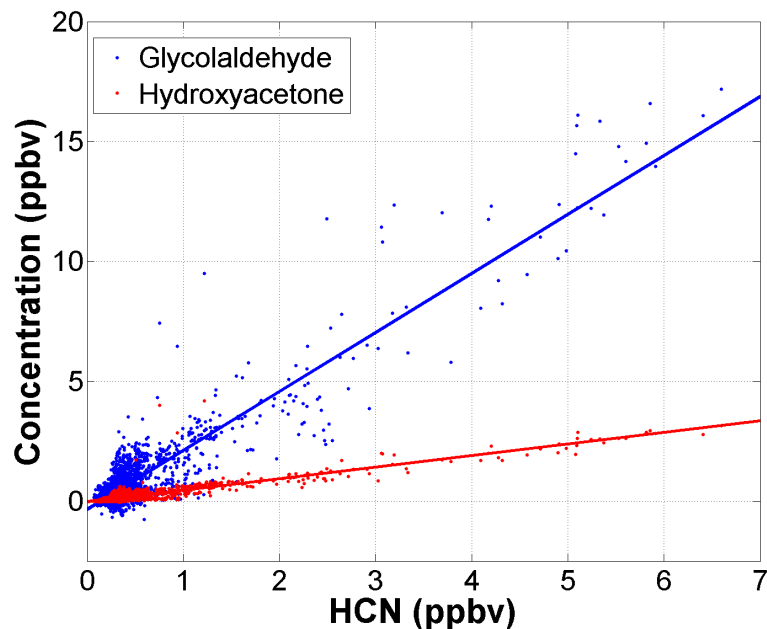
Fig. 7. Correlation between glycolaldehyde and HCN (blue) and hydroxyacetone and HCN (red) during the ARCTAS-CARB 2008 campaign. The slope of the linear regression is 2.5 and 0.48, respectively. $R^2 = 0.84$ and 0.77, respectively.
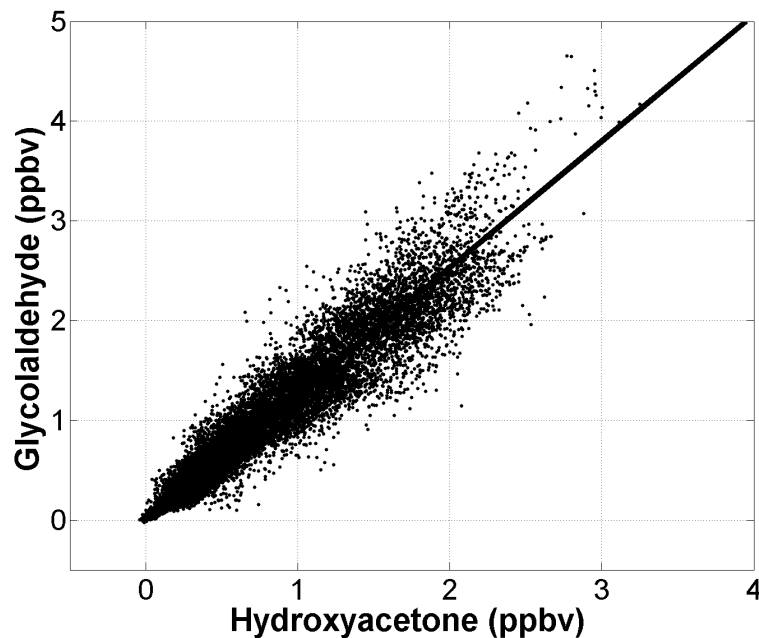
Fig. 8. Correlation between glycolaldehyde and hydroxyacetone during the BEARPEX 2009 campaign. The slope of the linear regression is 1.3, and the intercept is 0.70 pptv. $R^2 = 0.91$. The correlation is consistent with the hypothesis that hydroxyacetone and glycolaldehyde have similar sources and sinks.

Title Page

Abstract   Introduction

Conclusions   References

Tables   Figures

◄◄   ►►

◄   ►

Back   Close

Full Screen / Esc

Printer-friendly Version

Interactive Discussion

A.

Production of Glycolaldehyde / Production of Hydroxyacetone
Isoprene
MBO

Production of Glycolaldehyde / Production of Hydroxyacetone

Concentration (ppbv)

Model Time (min)

B.

Sacramento

BEARPEX

Glycolaldehyde / Hydroxyacetone
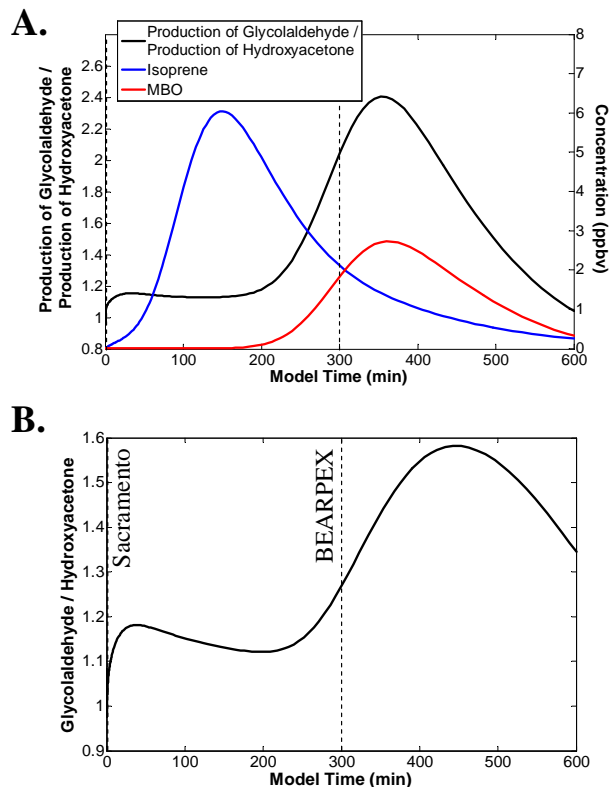
Model Time (min)

Fig. 9. Ratio of the production of glycolaldehyde to the production of hydroxyacetone and concentration of isoprene and MBO **(A)** as predicted by a simple box model of the BEARPEX 2009 campaign. Ratio of glycolaldehyde concentration to hydroxyacetone concentration **(B)**. As the BEARPEX site is approximately five hours downwind of Sacramento, CA, model oxidation time of 300 min is expected to correspond to site conditions.